

An Automatic Technique for MRI Based Murine Abdominal Fat Measurement

Yang TANG¹, Richard SIMERLY², Rex A. MOATS¹

¹Dept. of Radiology, Children's Hospital Los Angeles, Univ. of Southern California, 4650 Sunset Blvd., Los Angeles, USA

²Dept. of Pediatrics, Children's Hospital Los Angeles, Univ. of Southern California, 4650 Sunset Blvd., Los Angeles, USA

yangt.chla@gmail.com

Abstract. *Because of the well-known relationship between obesity and high incidence of diseases, fat related research using mice models is being widely investigated in preclinical experiments. In the present study, we developed a technique to automatically measure mice abdominal adipose volume and determine the depot locations using Magnetic Resonance Imaging (MRI). Our technique includes an innovative method to detect fat tissues from MR images which not only utilizes the T1 weighted intensity information, but also takes advantage of the transverse relaxation time(T2) calculated from the multiple echo data. The technique contains both a fat optimized MRI imaging acquisition protocol that works well at 7T and a newly designed post processing methodology that can automatically accomplish the fat extraction and depot recognition without user intervention in the segmentation procedure. The post processing methodology has been integrated into easy-to-use software that we have made available via free download. The method was validated by comparing automated results with two independent manual analyses in 26 mice exhibiting different fat ratios from the obesity research project. The comparison confirms a close agreement between the results in total adipose tissue size and voxel-by-voxel overlaps.*

Keywords

Measurement, MRI, abdominal, mice, FatExtractor.

1. Introduction

The increased incidence of obesity and well-documented co-morbidities, have lead to the recognition that obesity is a public health epidemic [1], [2]. Researchers studying adipose tissue and the associated disease processes are actively pursuing preclinical studies using mouse models [3], [4]. In obesity research, the assessment of change in adipose tissue is an important measure of metabolic dysfunction that is often repeatedly performed during longitudinal experiments.

Small Animal MRI is a powerful tool for in vivo fat measurement and can provide quantitative information

about fat volume as well as depot locations [5]. However, for quantitative analysis MR images require extensive manual measures, especially for large 3D datasets involving temporal assessment. Fat measurement can be aided by automated and semi-automated techniques relieving the researcher the tedious operational burdens and reducing the operator-dependent bias and errors.

Performing automatic measurements requires that two issues be addressed.

First, the fat tissues must be segmented from the background and other tissues in the acquired MRI images. Because fat is relative bright in T1 weighted images, this issue is often addressed by applying the threshold to the intensities [5-7]. Thresholding works for uniform images, but for high field MR images, the variance of intensities caused by instrument is often too large to be ignored. One solution to deal with the variance is to set the threshold locally [6] or adaptively [7]. Solutions using fuzzy logic methods have also been applied. In these cases, each pixel is assigned a fuzzy membership to indicate the probability that the pixel is fat. Then the fat is extracted by minimizing the membership function instead of being based solely on a threshold [8], [9]. More mathematically complex models have been created to compensate for the inhomogeneities in the intensity images [10], [11]. But methods based only on intensity are in general limited because other tissues or objects in the background exhibit similar intensities and are thus indistinguishable. As a result, image acquisition techniques have been proposed to provide better discrimination. The water-saturation technique [12-14] performs well on the human fat evaluation. However, these have not been implemented for small animals at high field strengths (7T and above) due to magnetic field inhomogeneities at high field that can lead to artifacts and due to the increased difficulty of implementing strictly analogous acquisition techniques.

The second important issue in fat analysis is to assign the fat depot type to associated anatomical location including subcutaneous fat and visceral fat. Fat location has been shown to be an important factor in obesity-associated morbidity [15], [16]. A common method useful for the fat depot recognition is region growing [5], [6], which starts from seed points planted in each different fat depots and

sorts nearby pixels with similar intensities. To separate the visceral and subcutaneous fat, curve deformation methods [8], [9], [17] have also been adopted. These methods deform a curve inwards from skin contour to locate a muscle layer. Because the muscle layer lies between the subcutaneous and visceral fat, the different fat depots are separated by default. However, in our hands, we find that these methods do not work well for the thin mice with less fat usually in the early stage of increasing adiposity. Because in the skinny mice, the sparse and separated adipose depots complicate the automatic placement of seeds for region growing methods, and the muscle layer is not obvious to locate the deformed curves.

Although the fat measurements using imaging technique has been established in humans [6], [18] at lower field strengths, fat measurement in mice models using MRI has not been adequately addressed. To improve image acquisition, we utilize information from the transverse relaxation time (T2) determined from multi echo data. In our method, the fat extraction is accomplished by adopting a fuzzy c mean clustering algorithm in the T1 weighted image and then selecting clusters into fat regions aided by the additional T2 information. To complement this image acquisition related information, we developed a depot recognition method which utilizes a knowledge-based framework for image post acquisition image processing. This methodology takes advantages of the a priori anatomical knowledge and automatically segments each depot into visceral fat or subcutaneous fat using fuzzy inference schemes.

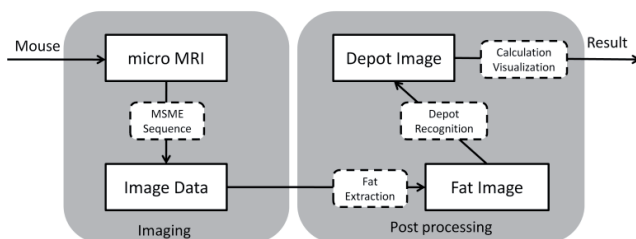


Fig. 1. The workflow of automatic technique.

Herein, we describe a technique for automatic mice abdominal fat measurement using MRI, which includes both an image acquisition protocol and a post processing methodology (Fig. 1). The post processing algorithms of the technique were implemented in user-friendly software '*FatExtractor*' (tool and documents are freely available at the <http://code.google.com/p/fat-extractor>), which generally includes following functions: (1) automatic estimation and measurement of the fat tissues. (2) automatic separation and measurement of visceral and subcutaneous fat depots. (3) batch processing for volume dataset. (4) parameters customization for different applications. We developed a novel quantitative framework in this study and hope it to be helpful to adipose research groups.

2. Materials and Methods

2.1 Imaging Protocol

Mice were scanned on the small animal MRI scanner (70/16 Bruker PharmaScan, Germany). The field strength is 7.05 Tesla and the maximal gradient strength is 400 mTesla/m. Mice were placed prone in a semi cylindrical holder inserting into a coil with inner 3.8cm volume coil diameter. To capture the images in a defined reproducible region of abdomen, the scan started at the top of the left kidney and ends at the end of right kidney. In previous research [19], the abdominal region has been defined from L1 to L5 according to the spine in the CT images. While in the MR modality, bone is not as easily differentiated as it is in the CT modality. Thus, in this study, we utilized the kidneys as the anatomical landmarks to define our abdominal volume of interest.

To provide adequate signal to noise and coverage, about 15 slices were collected in the abdominal region with 1mm slice thickness. Based on our experience, multi echo spin sequences at 7T offer an optimal combination of resolution, acquisition time, robustness, and reproducibility in what tends to be a technically challenging environment in MRI terms. A Bruker multiple-slice-multiple-echo (MSME) sequence (TR = 5300 ms, TE = 12~120 ms, 10 echoes) was adopted. These acquisition parameters were optimized empirically to provide good contrast and the shortest practical TR. The TR, which affects T1 contrast as well as total signal, and the effective T2, which is directly affected by the number of slices, were empirically determined to provide optimal contrast at the shortest reasonable scan time while maintaining a useful field of view. The exact optimization procedure was quite involved and is beyond the scope of the current manuscript. The field of view was 3*3cm and matrix size was 256*256, in-plane resolution 117 μ m. All experiments were conducted under the principles of CHLA IUCAC.

2.2 Post Processing Procedures

To accomplish the automatic adipose measurement, two tasks were performed: fat extraction and depot recognition. Prior to the fat extraction, a bilateral filter [20] was applied to the image data to increase the effective signal to noise ratio (SNR) without significantly degrading the quality of the images.

2.2.1 Fat Extraction

The basic methodology is illustrated in Fig. 2. First, a T2 parametric image is calculated from the multiple echo images. Then, a cluster algorithm is applied to the intensity information in the first echo image allowing the classification of all pixels into different clusters. Finally, the clusters with average T2 values similar to those of the fat tissues are defined and extracted as fat tissue.

(a) Cluster Image

The initial choice to use of the first echo image proved to be expeditious because of its relatively high SNR compared to later echo images. In the first step, instead an explicit threshold, the fuzzy c means (FCM) clustering approach [21] was adopted to classify all pixels into groups and produce a cluster image.

The cluster number is an important parameter in clustering approaches. In the previous research [5], [8], [9], the cluster number was usually defined to be three, corresponding to background, fat and muscles. Nevertheless, in the real anatomy, more organs and tissues are included in the MR image. Three clusters cannot well describe the discrepancies between different tissues. Increasing the cluster number was necessary to more accurately describe the full data. The fat tissue may display in multiple clusters and it becomes difficult to correctly select the appropriate cluster using intensity-only images. In our method, the clusters are recognized by their T2 values, which allowed us to increase the number of clusters. In the *FatExtractor*, five is set as the default based on our experience.

(b) T2 parametric image

The T2 value is independent of intensity and reflects the inherent character of each tissue. Thus, the information from the T2 parametric image can help us to discriminate between clusters with similar intensities. An example is given in Fig. 3, demonstrating that the T2 parametric image shows more obvious discrimination between fat and nonfat than in the first echo image alone, thus providing the additional information useful in distinguishing the fat from the non-fat.

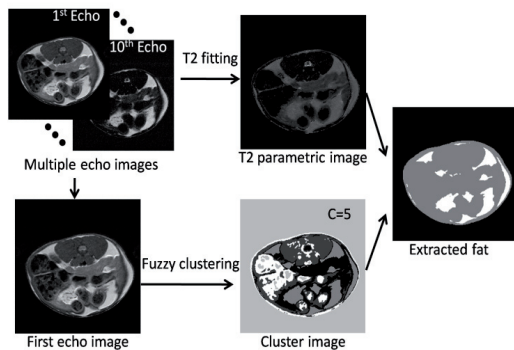


Fig. 2. Extraction of the fat tissues.

To calculate the T2 parametric image, the mono-exponential physical model is utilized, which has been adopted previously [22], [23], [24].

$$S_i(S_0, T_2) = S_0 \exp(-Te_i / T_2) \quad (1)$$

where S_i is the intensity in the i th echo, Te_i is the Te time in the i th echo and S_0 is the pseudo-proton density. The model presents a decay curve and the T_2 value can be calculated by fitting the multiple echo data to the curve.

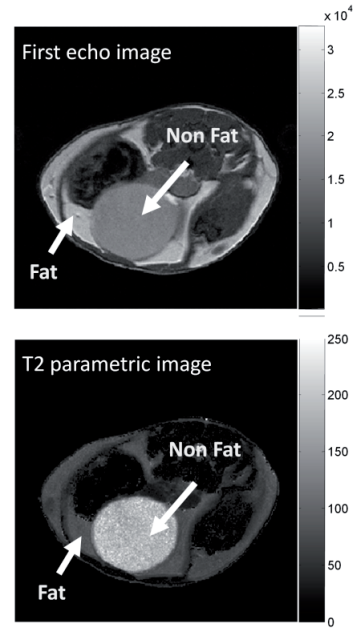


Fig. 3. An example of the difference between first echo image and a T2 parametric image.

In our method, the least square algorithm is used for curve fitting and the Marquardt-Levenberg algorithm [25] is selected for the optimization. To decrease the affection of noise, the baseline subtraction [26], [27] is applied and the fitting points with their intensities under the baseline are discarded. Therefore, only the reliable T2 value are calculated and those pixels with less than a given number of points less than a threshold (set as 5 in our 10 echoes protocol) are kept empty (set to 0) in the T2 parametric image.

(c) Fat extraction with T2 reference

The fat regions are extracted in the cluster image by comparing the clusters' similarities in T2 values. Using the T2 parametric images, the average T2 values are calculated for each cluster. A similarity threshold T_s is defined as following.

$$T_s = |T_{2\text{cluster}} - T_{2\text{fat}}| / T_{2\text{fat}} \quad (2)$$

Here the $T_{2\text{cluster}}$ is the average T2 value in each cluster from non-empty pixels and $T_{2\text{fat}}$ is the T2 value of fat.

Because the T2 value is related to the magnetic field strength, the $T_{2\text{fat}}$ is suggested to be defined by drawing a ROI in the known fat region using the exact same imaging protocol and instrument.

The similarity threshold in (2) defines a T2 range. The clusters with T2 value in the defined range are considered as fat tissues. Because the T2 values of fat and non-fat tissues are generally distinguishable, the threshold can be set according to the each application. In our system at 7T $T_s = 15\%$ works well. To allow for difference in experimental designs, the $T_{2\text{fat}}$ and T_s are adjustable in the software tool.

2.2.2 Fat Depot Recognition

The basic procedures for the recognition method are illustrated in Fig. 4. Before the knowledge is applied, a morphological operation is performed to decompose the fat tissues. Then the unconnected parts are labeled and a knowledge-based method is applied to recognize each object into visceral or subcutaneous fat.

In the decomposition step, a morphological open operation [28] is employed on the fat image, which separates the neighboring tissues that have incidental contact. This open operation step has the property of excluding small areas associated with the incidental contact. Rather than discarding these regions, we save them as small independent regions that are later evaluated for depot recognition.

After decomposition, unconnected fat tissue are labeled as individual regions in the label image as shown in Fig. 4. To sort these individual regions into their likely respective fat depots, we employ the anatomical features, which are described by 4 parameters. To allow for uncertainty caused by anatomical variance, the parameters are expressed by fuzzy logic [31] which is assigned a confidence score using a membership function between 0 and 1.

(a) Parameters

Parameter 1: Orientation

Previous research indicates that the abdominal fat in mice tends to accumulate in a bilateral pattern [30]. Taking advantage of this a priori information, we implemented an orientation parameter dividing the body into bilateral regions and dorsal/ventral regions (Fig. 5a). The orientation

parameter for each individual region in a polar system with its origin located at the geometrical centroid of the body area is as the mean of the maximum and minimum angles (Fig. 5b).

$$\text{Orientation} = (\text{maximum angle} + \text{minimum angle})/2$$

Parameter 2: Minimum distance

We define a feature of location, for each pixel inside the body area which represents its distance to the nearest body contour. As Fig. 5a shows, a distance map is displayed for the inside body area with the intensity corresponding to the distance. For example, the bright pixel near the centroid denotes a long distance to the body contour. The exact steps to obtain distance map are described in Appendix A.

The minimum distance parameter describes how close the outer edge of the fat region is to the body surface and is defined as the minimum value of the distance map in an individual region. This parameter is important for distinguishing the subcutaneous from visceral fat.

Parameter 3: Maximum distance

Similar with minimum distance, maximum distance is used to express the location feature that describes how far the fat tissues are away from the body surface. It is defined as the maximum value of the distance map in an individual region. Both minimum distance and maximum distance have three membership functions defining a confidence score for small, medium and large distance (Fig. 5c). Taking into consideration the observed regional variances [30], the range defined as small in the bilateral region is wider than the dorsal/ventral region.

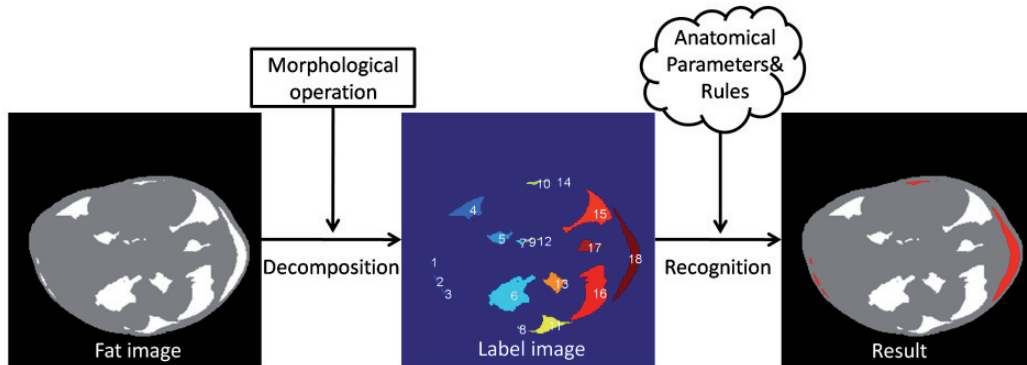


Fig. 4. The procedures of depot recognition.

Parameter 4: Elongatedness

Elongatedness describes the shape of the object. Derived from empirical observations, in the band-like region near the body surface, the subcutaneous fat segments are usually slender along the surface and this a priori shape information is exploited in the location feature. An elongatedness parameter is defined to be the ratio of the length to thickness (Fig. 5b):

$$\text{Elongatedness} = \text{length} / \text{thickness}$$

where (length = maximum angle - minimum angle) and (thickness = maximum distance - minimum distance).

(b) Fuzzy inference

Utilizing the defined parameters, the depot can be recognized by classical If-Then rules and a min-max fuzzy inference scheme. Tissues are assigned to either the bilateral region or dorsal/ventral region according to their orientations. Then three rules are employed to distinguish the depots:

Rule 1: If the maximum distance is small, then it is subcutaneous fat.

Rule 2: If the minimum distance OR the maximum distance is large, then it is visceral fat.

Rule 3: If the minimum distance is small AND the maximum distance is medium AND the shape is elongated, then it is subcutaneous fat.

With the defined rules, the min-max fuzzy inference scheme will automatically calculate the weights for each rule and assign the depot type in term of the weighted centroid [29].

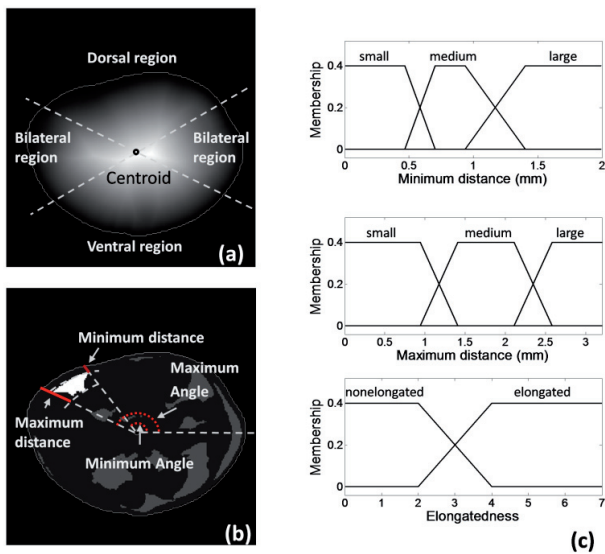


Fig. 5. The description of the parameters. (a) The distance map and regional divisions. (b) Parameter indications based on anatomical knowledge. (c) Example of fuzzy logical representation of the knowledge contained in the bilateral regions.

3. Experiments and Results

To demonstrate and validate our technique, we present the results of methodology analyzed in an actual obesity experiment performed in 26 wild type C57BL/6 mice.

In the adipose experiment, mice were separated into 4 groups differentiated by feeding strategies. Mice received regular chow or a high fat diet respectively. In the regular chow group, mice were placed into 3 litters with different sibling numbers that provided different nutritional conditions due to competition or lack of competition. The details of animal experiments are listed in Tab. 1 including large litter (LL), normal litter (NL), small litters (SL) and high fat (HF) groups. The feeding strategies produce different amount of adipose tissue, which gave us the opportunity to test the performance of our methodology on mice with different adipose ratios.

In order to validate the performance, the proposed automatic analysis method was compared with manual

results from the animal in the described obesity experiments. The proposed automatic processing method implemented in Matlab 7.6 (MathWorks, Natick, MA, USA) environment. The manual results were segmented by the experienced technicians from Small Animal Imaging Research Center (SAIRC) of CHLA-USC. In each mouse, a typical slice in the abdominal region near the caudal end of the lower kidney is selected for manual segmentation and compared with automatic results, where both SAT and VAT are included.

| Group | Mouse num (Male, Female) | Feed | Little | Sibling num |
|-------|--------------------------|----------|----------|-------------|
| LL | M=6 F=1 | Chow | LL | 12 |
| NL | M=4 F=1 | Chow | NL | 7 |
| SL | M=7 F=2 | Chow | SL | 3 |
| HF | M=2 F=3 | High Fat | LL,NL,SL | 5 |

Tab. 1. Animal experiments.

In order to take inter-operator variations into account, two independent technicians performed the manual segmentations using a customized software tool developed in Matlab. In the software, two basic functions were provided including threshold and ROI. The technicians first select the fat regions by adjusting a threshold. Then multiple manual ROI operations were performed to add or delete the fat regions based on the users' experience. The total segmented fat is TAT. To segment the subcutaneous and visceral fat, operators carefully delineate a contour between these two types of depots. Finally, the fat inside the contour is considered as VAT and the rest of the fat is SAT.

Using automatic technique, the reconstructed 3D result of the extraction of abdominal fat depots from the 4 groups is demonstrated in Fig. 6.

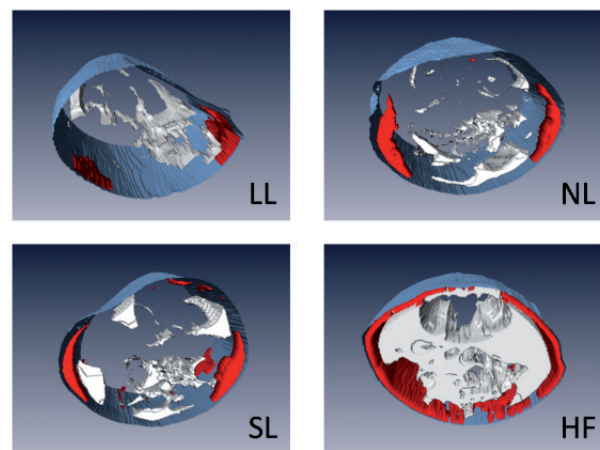


Fig. 6. Reconstructed results from 4 groups with different fat ratios.

For the time issue, the average processing time for each slice cost more than 5 minutes by manual operations, while for automatic processing, it is about 10 seconds.

The first comparison is for the segmented adipose size, which were performed in TAT, VAT and SAT respectively for all mice. A linear regression with 95% confi-

dence ($P < 0.001$) was calculated for each comparison. For the first manual result, the R^2 for TAT is 0.953 with the regression function $y = 1.088x + 0.4407$; R^2 for VAT is 0.9627 with the regression function $y = 1.058x + 1.769$; R^2 for SAT is 0.8221 with the regression function $y = 1.042x + 0.8719$. For the second manual result, the R^2 for TAT is 0.912 with the regression function $y = 1.009x + 6.583$; R^2 for VAT is 0.9154 with the regression function $y = 0.9889x + 6.924$; R^2 for SAT is 0.8986 with the regression function $y = 1.037x + 0.3821$. The agreement in the R^2 value denotes the linear relationship between the automatic and manual results, and the concordance in the slope of the function provides confidence that the relationship will hold true in a variety of conditions. The agreement between the automatic results and manual results is comparable to the difference between correlation coefficients of the two manual results, which for TAT: $R^2=0.9514$, VAT: $R^2=0.9195$ and SAT: $R^2=0.8767$.

A second comparison was performed to evaluate the voxel-by-voxel overlap of the segmented TAT, SAT and VAT respectively. To qualify these spatial similarities, we adopted the dice coefficient which is customarily used to compare the segmentation results in medical imaging.

As equation (3) shows, the Dice Coefficient (DC) describes the average ratio of the intersection between the results (R1) and results (R2). For example, a complete overlap of the segment results will make the DC to be 1.

$$DC = \frac{2|R_1 \cap R_2|}{|R_1| + |R_2|} \quad (3)$$

We calculated the DC in the 26 mice for TAT, VAT and SAT respectively. The average value between automatic result and two manual results are for TAT: $DC = 0.8839$, for VAT: $DC = 0.8795$ and for SAT: $DC = 0.873$. The detailed statistic DC value (mean value \pm standard deviation) for each result is displayed in Tab. 2.

| DC | TAT | VAT | SAT |
|----------|---------------------|---------------------|---------------------|
| A vs. M1 | 0.9087 \pm 0.0438 | 0.8999 \pm 0.0467 | 0.8783 \pm 0.0546 |
| A vs. M2 | 0.8591 \pm 0.0558 | 0.840 \pm 0.0634 | 0.8677 \pm 0.0435 |
| M1 Vs.M2 | 0.8846 \pm 0.052 | 0.8717 \pm 0.0598 | 0.8847 \pm 0.0491 |

Tab. 2. Dice Coefficient (DC) of automatic (A), first manual result (M1) and second manual result (M2).

4. Discussion

This study presents an automatic technique for abdominal fat measurement in mice models, which has been reported to be closely correlated to the total amount of body fat in small animal [19] and directly related to many diseases [2], [16].

Different from existing MRI fat assessment methods [5-9], we have created a new way to detect the fat not only based on image intensities, but also taking into consideration the transverse relaxation time using a multiple spin echo sequences. The T2 combination method increases the ability to distinguish the pixels with similar intensities into fat and non-fat. In contrast to other segmentation based

clustering techniques [5], [8], [9], our method is relatively insensitive to the predefined cluster number which allows for more clusters and more accurate segmentation.

Another difference between early techniques and ours lies in the procedures for depot recognition. Instead of a region growing or curve deformation, a knowledge-based framework has been adopted in our fat depot analysis that is better suited for analyzing mice with varying fat ratios. We used the fuzzy sets to express the anatomical knowledge and make inference by rules to distinguish the subcutaneous fat from visceral fat. Such a framework is intuitive and flexible allowing researchers to apply it to other problems.

We designed and implemented our method for images acquired at 7T MRI, but it can be applied to other magnetic field strengths. Because the T2 value is related to the basic magnetic field intensities, users must set the predefined fat T2 value according to their applications. Thus, the parameters are customizable in the *FatExtractor*.

In the current method, orientation was considered as one of the feature parameters. To calibrate the orientation, all the mice must be placed prone in the holder in the experiments (small rotation is not significant but larger ones are). In the next version of the software, we will allow the user to adjust the knowledge for customized applications. For example, change the scale of maximum and minimum distances to be applied in puppies. The advantage of using a knowledge-based framework is that it can be extended in the future to include new anatomical structures including different definition of the fat depots. For example, isolation of organs can be added to compose a semantic network [32] for further refinement of the definitions of the fat depots.

In our subsequent interactions with fat research groups, we have noted a desire for processing that can automatically match each fat tissue to adjacent organs. For this purpose, the atlas-based technique [34] is a good choice. With a mouse atlas, each organ in the abdominal region can be registered and how abdominal fat tissues relate to these organs may be determined. However, creating a technique for aligning an atlas to mice with less predictable adipose tissue will require a challenging and exacting methodology to be created and tested. We may also implement a fat-water separation technique applicable at 7T. Groups working in the field will likely produce sequences that allow the efficient separation of fat signals in MRI.

In conclusion, we have developed a quantitative framework for abdominal fat measurement in a mouse model using MRI. We have presented the imaging protocol and technical detail of the post-processing methodology in this paper. Software implementing our framework is downloadable from the project website. The parameters are well defined yet adjustable and tunable to new applications. By decreasing the amount of manual operation needed, we hope this technique can reduce the threshold for obesity researchers to use MRI in their research.

5. Competing Interests Statement

The authors declare no competing interests.

Appendix A: Distance Map

To obtain the distance map, couples of steps are carried out. As Fig. 7 shows, the first step is to get the mouse body mask. The threshold method is utilized to segment the body region from the background. Because the background is obviously dark in the T1 weight image, the threshold is not very sensitive. In our experiments, background threshold $T_{bkg} = 10\% \sim 15\%$ works well for our data, which means the clusters with their average intensity less than T_{bkg} of the maximum intensity are considered as background. After thresholding, a morphological hole filling [28] is performed to fill the small holes inside the body area. The body mask shows to be a connected region in the binary image.

In body mask image, the surface contour corresponds to the boundary of the mask. In the binary image, the Moore-Neighbor boundary-tracing algorithm [28] is used to produce the surface contour.

To calculate the Euclidean distance from each pixel to the nearest surface contour, the Euclidean transform [34] is performed and the distance map is obtained.

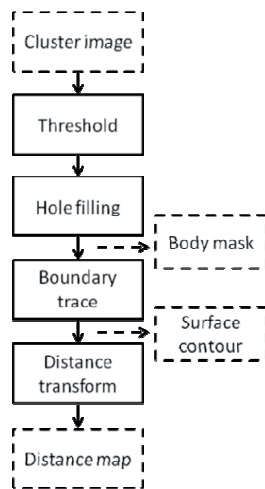


Fig. 7. Steps to calculate the distance map.

References

- [1] MANN, G. V. The influence of obesity in health. *N Engl J Med*, 1974, vol. 291, p.178–185.
- [2] LARSSON, B., SVÄRDSUDD, K., WELIN, L., WILHELMSSEN, L., BJÖRNTORP, P., TLIBBLIN, G. Abdominal adipose tissue distribution, obesity and risk of cardiovascular disease and death: 13 y follow up of participants in the study of men born in 1913. *Br Med J Clin Res*, 1984, vol. 288, p.1401-1404.
- [3] BECHAH, Y., PADDOCK, C. D., CAPO, C., MEGE, J. L., RAOULT, D. Adipose tissue serves as a reservoir for recrudescing *Rickettsia prowazekii* infection in a mouse model. *PLoS One*, 2010, vol. 5, no. 1, e. 8547.
- [4] CHURCH, C., LEE, S., BAGG, E. A., MCTAGGART, J. S., DEACON, R., GERKEN, T., LEE, A., MOIR, L., MECINOVIĆ, J., QUWAILID, M. M., SCHOFIELD, C. J., ASHCROFT, F. M., COX, R. D. A mouse model for the metabolic effects of the human fat mass and obesity associated FTO gene. *PLoS Genet*, 2009, vol. 5, no. 8, e. 1000599.
- [5] RANEFALL, P., BIDAR, A. W., HOCKINGS, P. D. Automatic segmentation of intra-abdominal and subcutaneous adipose tissue in 3D whole Mouse MRI. *J Magn Reson Imaging*, 2009, vol. 30, no. 3, p. 554-560.
- [6] SIEGEL, M. J., HILDEBOLT, C. F., BAE, K. T., CHENG, H., WHITE, N. H. Total and intraabdominal fat distribution in preadolescents and adolescents: Measurement with MR imaging. *Radiology*, 2007, vol. 242, no. 3, p. 846-856.
- [7] CHAE, Y., JEONG, M. G., KIM, D. Three dimensional volume measurement of mice abdominal fat in magnetic resonance images. *e-Health Networking, Application and Services*, 2007, p. 252–255.
- [8] POSITANO, V., GASTALDELLI, A., SIRONI, A. M., SANTARELLI, M. F., LOMBARDI, M., LANDINI, L. An accurate and robust method for unsupervised assessment of abdominal fat by MRI. *J Magn Reson Imaging*, 2004, vol. 20, no. 4, p. 684-689.
- [9] POSITANO, V., CHRISTIANSEN, T., SANTARELLI, M. F., RINGGAARD, S., LANDINI, L., GASTALDELLI, A. Accurate segmentation of subcutaneous and intermuscular adipose tissue from MR images of thigh. *J Magn Reson Imaging*, 2009, vol. 29, p. 677-684.
- [10] HOU, Z. A review on mr image intensity inhomogeneity correction. *Int. J. Biomed. Imag*, 2006, p.1-11.
- [11] VOVK, U., PERNUŠ, F., LIKAR, B. A review of methods for correction of intensity inhomogeneity in MRI. *IEEE Trans Med Imaging*, 2007, vol. 26, p. 405–21.
- [12] DIXON, W. T. Simple proton spectroscopic imaging. *Radiology*, 1984, vol. 153, p. 189-194.
- [13] REEDER, S. B., PINEDA, A. R., WEN, Z., SHIMAKAWA, A., YU, H., BRITAIN, J. H., GOLD, G. E., BEAULIEU, C. H., PELC, N. J. Iterative decomposition of water and fat with echo asymmetry and Least-Squares Estimation (IDEAL): Application with fast spin-echo imaging. *Magnetic Resonance in Medicine*, 2005, vol. 54, p. 636–644.
- [14] PENG, Q., MCCOLL, R. W., WANG, J., CHIA, J. M., WEATHERALL, P. T. Water-saturated three-dimensional balanced steady-state free precession for fast abdominal fat quantification. *J Magn Reson Imaging*, 2005, vol. 21, p. 263–271.
- [15] MANSON, J. E., COLDITZ, G. A., STAMPFER, M. J., WILLETT, W. C., ROSNER, B., MONSON, R. R., SPEIZER, F. E., HENNEKENS, C. H. A prospective study of obesity and risk of coronary heart disease in women. *N Engl J Med*, 1990, vol. 322, p. 882–889.
- [16] LESLIE, W. D., LUDWIG, S. M., MORIN, S. Abdominal fat from spine dual-energy X-ray absorptiometry and risk for subsequent diabetes. *J Clin Endocrinol Metab*, 2010, vol. 95, no. 7, p. 3272-3276.
- [17] ZHAO, B., COLVILLE, J., KALAIGIAN, J., CURRAN, S., JIANG, L., KIJEWski, P., SCHWARTZ, L. H. Automated quantification of body fat distribution on volumetric computed tomography. *J Comput Assist Tomogr*, 2006, vol. 30, no. 5, p. 777 to 783.
- [18] OHSHIMA, S., YAMAMOTO, S., YAMAJI, T., SUZUKI, M., MUTOH, M., IWASAKI, M., SASAZUKI, S., KOTERA, K., TSUGANE, S., MURAMATSU, Y., MORIYAMA, N. Development of an automated 3D segmentation program for volume quantification of body fat distribution using CT. *Nippon Hoshasen Gijutsu Gakkai Zasshi*, 2008, vol. 64, no. 9, p. 1177-1181.
- [19] LUU, Y. K., LUBLINSKY, S., OZCIVICI, E., CAPILLA, E., PESSIN, J. E., RUBIN, C. T., JUDEX, S. In vivo quantification of

- subcutaneous and visceral adiposity by micro-computed tomography in a small animal model. *Med Eng Phys*, 2009, vol. 31, no. 1, p. 34-41.
- [20] TOMASI, C., MANDUCHI, R. Bilateral filtering for gray and color images. *Proc. Int. Conf. Computer Vision*, 1998, p. 839-846.
- [21] DUNN, J. C. A fuzzy relative of the ISODATA process and its use in detecting compact well-separated clusters. *Journal of Cybernetics*, 1973, vol. 3, p. 32-57.
- [22] LIU, J., NIEMINEN, A., KOENIG, J. L. Calculation of T1, T2 and proton spin density in nuclear magnetic resonance imaging. *Journal of Magnetic Resonance*, 1998, vol. 85, p. 95-110.
- [23] BONNY, J. M., ZANCA, M., BOIRE, J. Y., VEYRE, A. T2 maximum likelihood estimation from multiple spin-echo magnitude images. *Magnetic Resonance in Medicine*, 1996, vol. 36, p. 287-293.
- [24] SIJBERS, J., DEN DEKKER, A. J., VERHOYE, M., RAMAN, E., VAN DYCK, D. Optimal estimation of T2 maps from magnitude MR images. *Proc. SPIE Med. Imag.*, 1998, vol. 3338, p. 384.
- [25] MARQUARDT, D.W. An algorithm for Least-Squares estimation of nonlinear parameters. *Journal of the Society for Industrial and Applied Mathematics*, 1963, vol. 11, p. 431-441.
- [26] HENKELMAN, R. M. Measurement of signal intensities in the presence of noise in MR images. *Med. Phys*, 1985, vol. 12, p. 232 to 233.
- [27] YOUSEM, D. M., IHMEIDA, I., QUENCER, R., ATLAS, S. W. Paradoxically decreased signal intensity on post contrast short-TR MR images. *AJNR*, 1991, vol. 12, p. 875-880.
- [28] GONZALEZ, R. C., WOODS, R. E. *Digital Image Processing*. 2nd edition. Boston, MA: Addison-Wesley Longman Publishing, 1992.
- [29] ZADEH, L. A. Fuzzy sets. *Inform Contr*, 1965, vol. 8, p. 338-353.
- [30] CALDERAN, L., MARZOLA, P., NICOLATO, E., FABENE, P. F., MILANESE, C., BERNARDI, P., GIORDANO, A., CINTI, S., SBARBATI, A. In vivo phenotyping of ob/ob mouse by magnetic resonance imaging and H-Magnetic resonance spectroscopy. *Obesity*, 2006, vol. 14, p. 405-414.
- [31] COX, E. *The Fuzzy Systems Handbook: a Practitioner's Guide to Building, Using and Maintaining Fuzzy Systems*. Academic Press, 1994.
- [32] MINSKY, M. A framework for representing knowledge. In P.H. Winston(Ed), *The Psychology of Computer Vision*. New York: McGraw-Hill, 1975.
- [33] COLLINS, D. L., ZIJDENBOS, A. P., BAARÉ, WIM F. C., EVANS, A. C. Animal+Insect: Improved cortical structure segmentation. *Lecture Notes in Computer Science*, 1999, vol. 1613, p. 210-223.
- [34] CALVIN, M., QI, R. S., RAGHAVAN, V. A Linear time algorithm for computing exact Euclidean distance transforms of binary images in arbitrary dimensions. *IEEE Transactions on Pattern Analysis and Machine Intelligence*, 2003, vol. 25, no. 2, p. 265-270.

About Authors

Yang TANG received his B.E. and Ph.D. degrees in Computer Science from Nanjing University of Technology and Science in 2001 and 2006 respectively. From 2008, he joined the Children's Hospital Los Angeles, affiliated with the Keck School of Medicine, University of Southern California as a research fellow. His research interests include medical application via computer image and graphic techniques.

Richard SIMERLY received his A.B. from UC Berkeley in 1976 and Ph.D. from UCLA in 1984. His research topics include the axon targeting in limbic and hypothalamic neural pathways, leptin receptor signaling in developing hypothalamic circuitry and development of sexually dimorphic forebrain regions. He is professor of pediatrics at the Keck School of Medicine, University of Southern California, deputy director of the Saban Research Institute, Children's Hospital Los Angeles, and director of its developmental neuroscience program.

Rex A. MOATS was born in Montana, USA. He received his B.S. and Ph.D. degrees from Montana State University in 1984 and 1990 respectively. After that, he joined the Department of Chemistry, California Institute of Technology as a research fellow. His research interesting includes imaging agent development and quantitative methods of image acquisition and analysis. He now is the assistant professor at the Keck School of Medicine, University of Southern California and the director of Small Animal Imaging Research Center, Children's Hospital Los Angeles.